Fractal structure of silica colloids revisited

Tomàs Sintes†, Raúl Toral†‡ and Amitabha Chakrabarti§

† Departament de Física, Universitat de les Illes Balears, E-07071 Palma de Mallorca, Spain
‡ Instituto Mediterraneo de Estudios Avanzados, IMEDEA (CSIC-UIB), E-07071 Palma de Mallorca, Spain
§ Department of Physics, Kansas State University, Manhattan, KS 66506, USA

Abstract. We present extensive computer simulations of a modified Eden model on a tetragonal lattice. This model is able to reproduce the crossover from mass fractal to surface fractal structures observed experimentally in the clustering process of partially hydrolysed silica particles.

One of the most interesting phenomena in random growth is that systems with only short-range interactions can form aggregates whose large-scale structures are statistically well defined. Many of these structures can be described as mass fractals or surface fractals. [1, 2]. For mass fractals, the mass (M) and the corresponding radius of gyration (R) obey the scaling relationship: $M \sim R^{D_f}$ where D_f is the fractal dimension; $1 \leqslant D_f < d$. In contrast to mass fractals, the mass of a surface fractal scales with the radius in a Euclidean fashion ($D_f = d$), but the surface area S now increases with the radius more rapidly: $S \sim R^{D_s}$; $d - 1 \leqslant D_s < d$.

Scattering experiments are used to quantitatively determine the structure of such systems. For mass fractals, the scattering intensity as a function of wavevectors, $I(k)$, shows a power-law behaviour for large k given by [3]

$$I(k) \sim k^{-D_f}$$

except for the case $D_f \to d$, when instead we obtain the asymptotic form $I(k) \sim k^{-(d+1)}$ which is Porod's law [4, 5]. For surface fractals, the scattering from the bulk is parallel to the incident beam, and the scattering at finite angles arises only from the surface. In this case, the scattering intensity follows a power law [6]

$$I(k) \sim k^{D_s - 2d}.$$

Thus, scattering measurements can distinguish between mass fractals, whose scattering curves, when plotted on a log–log scale, will be straight lines with slopes lying between -1 and -3, for a three-dimensional system, while the scattering curves for surface fractals will have slopes larger than -3.

Ceramic precursors are a typical example of systems that exhibit a variety of random structures. These range from highly ramified fractal objects to homogeneous colloidal particles with fractally rough surfaces [7, 8]. A prototypical example which we now describe in detail is a particular silica species, of chemical formula $(SiOC_2H_5)_{4-n}(OH)_n$, $1 \leqslant n \leqslant 4$, that grows in solution by condensation of partially hydrolysed silicon tetraethoxide (TEOS).

This silica is an *n*-functional monomer which can form *n* Si–O–Si linkages [9]. The silica polymerization proceeds in two steps: in the first step, functional sites (–SiOH groups) are generated by hydrolysis of TEOS in alkaline ethanol solution:

$$Si(OC_2H_5)_{4-(n-1)}(OH)_{n-1} + H_2O \rightarrow Si(OC_2H_5)_{4-n}(OH)_n + C_2H_5OH.$$
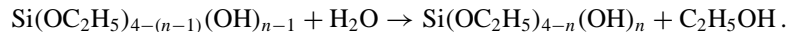
In the second step, silica polymers result from condensation of the hydrolysed species produced in the previous reaction:

$$R_k Si(OH) + R_l Si(OH) \rightarrow R_k Si\text{–}O\text{–}Si R_l + H_2O.$$
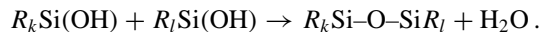
Those functional sites which remain unhydrolysed are called 'poisoned' and cannot mediate the polymerization reaction. It is possible to vary the functionality number distribution of hydrolysed sites by changing the [H_2O]:(TEOS) molecular concentration ratio (*W*) and as a consequence, morphologically different structures are generated. Experiments carried out on these systems [10, 11] with molar ratios ranging from $W = 1$ to $W = 4$ showed that for $W = 1$ the scattering curves exhibit a power-law behaviour consistent with a mass fractal description, while for $W \geqslant 2$ they were characteristic of surface fractals.

In a basic solution, silica undergoes condensation by a nucleophilic substitution mechanism that favours the reaction between the more acidic functional groups of the monomers with the more basic groups on the highly polymerized units [12]. The essential process is, therefore, one-particle nucleation that grows from monomers with all growth sites equally probable. The growth of the particles is reaction, rather than diffusion limited, as evidenced by the fact that particle growth occurs in several hours or a few days even in highly hydrolysed systems, whereas the typical time in diffusion-limited reactions is much smaller. In these processes the probability of a monomer attaching to a cluster is low with respect to the frequency with which it encounters the cluster. All potential growth sites are sampled by monomers, and the probability of attachment is determined by the local structure rather than the large-scale structure which governs the probability that a monomer encounters a given site.

A growth model which incorporates these two essential features, nucleation and chemically limited growth, is the Eden model [13]. In the Eden model growth occurs on a lattice by addition of monomers to randomly chosen surface sites starting from a nucleus. However, because of the incomplete hydrolysis of silica monomers, a fraction of the bonds is permanently poisoned and growth takes place only on the unpoisoned growth sites. Keefer and Schaefer [10, 11] developed a modified Eden model to simulate the formation of silica colloids on a two-dimensional square lattice in order to demonstrate the correlation between water concentration and fractal dimension. Subsequently, similar 'poisoned'-Eden models have been used by other authors [14, 15] to study growth and structures of various heterogeneous materials. However, in the two-dimensional model of Keefer and Schaefer, a site on the lattice was allowed to be poisoned by different silica monomers many times [11, 16] when incorporated to the aggregate. This leads to an unphysical situation which dramatically affects the morphology of the structures obtained and, as a consequence, the measure of the fractal dimension. Besides, no relation between the experimental ratio *W* and the mean functionality of the silica monomers was considered.

The purpose of this paper is to develop a model which accurately reproduces the geometry of the silica structure. In this model only empty sites on the lattice can be declared growth sites, as usual (containing an –OH group) and the other ones can be occupied only once by either a silica atom or a –OC_2H_5 group. The latter represent the poisoned sites. We will demonstrate, in a quantitative fashion, that incomplete hydrolysis is responsible for the development of fractal surfaces and the crossover to mass fractal as observed in

the experiments. We will find an algebraic relation between W and the mean number of hydrolysed sites per molecule contained in the structure, its mean functionality, from basic probabilistic arguments.

In our simulation we have considered a cell of dimensions $L \times L \times L$, where $L = 64$ lattice units. The silica aggregate structure can be regarded then as a *face centred cubic* lattice with two-point basis at $\boldsymbol{a} = \boldsymbol{0}$ and $\boldsymbol{b} = \frac{1}{4}(\boldsymbol{x} + \boldsymbol{y} + \boldsymbol{z})$. The vertices reproduce the structure of a regular tetrahedron and the coordination number is 4. The nearest neighbours of a point located at the point basis $\boldsymbol{a}$ are the four nearest points on point basis $\boldsymbol{b}$ and vice versa. The choice of a tetragonal lattice is a more natural choice for studying aggregation of silica monomers [7, 8]. Chemically limited nucleation and growth from incompletely hydrolysed monomers are simulated by a modification of the original rules of the Eden model: when a growth site is occupied, instead of designating all of the adjacent vacant sites as new growth sites, some of them are poisoned and are hence prohibited to be occupied. This aims to mimic the growth process explained earlier.

The simulation starts by placing a completely hydrolysed silica monomer at the centre of the cubic cell. Therefore, in the beginning, all four nearest neighbours become growth sites. Growth from a specified distribution of partially hydrolysed species is simulated by picking in advance the number of sites on the monomer which will be poisoned, the exact number chosen at random, but with a probability determined by a given distribution. Once one partially hydrolysed monomer is selected, the available growth sites of the cluster are then examined at random. If the selected growth site has a number of vacant or growth adjacent sites equal or greater than the number of poisoned sites on the monomer, that site is occupied. The vacant or growth adjacent sites are then poisoned at random, the sites that are left, if any, becoming new growth sites. If the number of growth sites on the cluster drops to zero, the cluster is declared 'dead'. If the number of growth sites is not zero, but there is no site which can accommodate the particular functionality of the chosen monomer we try again with another monomer of different functionality for which there are growth sites available. This situation is physically reasonable and in practice the number of monomers thrown back is very small compared to the total mass and does not alter the original distribution.

Once a cluster with the prescribed number of monomers has been grown, we compute the static structure factor, $S(\boldsymbol{k})$, which is proportional to the scattering intensity, $I(k)$,

$$S(\boldsymbol{k}) = \left\langle \frac{1}{N} \sum_{\boldsymbol{r}} e^{i\boldsymbol{k}\cdot\boldsymbol{r}} \sum_{\boldsymbol{r}'} \left[\nu(\boldsymbol{r} + \boldsymbol{r}')\nu(\boldsymbol{r}') - \langle\nu\rangle^2 \right] \right\rangle \tag{1}$$

where $\nu(\boldsymbol{r})$ is the number of monomers having the integer part of their coordinates equal to the lattice vertex $\boldsymbol{r}$, and $N = L^3$. Since we expect the aggregation process to be isotropic we compute the circularly averaged structure factor $S(k)$. Data have been finally averaged over one hundred different realizations. As explained earlier, the large-k behaviour of $S(k)$ has the form

$$S(k) \sim k^{-\alpha}$$

where structures with $1 \leqslant \alpha < 3$ correspond to mass fractals with $D_f = \alpha$, whereas $3 \leqslant \alpha < 4$ characterize a surface fractal with $D_s = 6 - \alpha$. We have kept this way for extracting the fractal exponents to allow a direct comparison with the experimental results of Keefer *et al* [10]. Although this might not be the most accurate of methods from a numerical point of view, the usual definition of the fractal dimension, which involves the radius of gyration, is not useful to distinguish surface fractal structures from smooth surfaces and it is also difficult to observe a crossover behaviour between mass and surface

fractals. Furthermore, the identification of external surfaces of a three-dimensional object is hampered by the presence of internal holes in the structure.

The structure of the clusters formed in this growth process is found to depend not only on the average functionality per monomer $\langle n \rangle$, but also on the distribution of these sites among the monomers, in particular, the RMS of the distribution, $\sigma(n)$. Here we present a systematic study for a whole set of tetra-, tri-, di-, and mono-functional monomer distributions, denoted as $f_4 : f_3 : f_2 : f_1$, with $0 \leqslant f_x \leqslant 3$ for $x = 1, 2, 3, 4$. We have performed simulations, for the complete set of parameters, for a prescribed number of particles per cluster of 10^4, 2.5×10^4, 5.0×10^4, and a few of them for 10^5 because of computer limitations. We have observed that the computed value of the fractal dimension, within the error bars, does not substantially change and does not show any tendency with the particle number. The results shown in the figures described below correspond to the case of 5.0×10^4 particles per cluster.

In figure 1 we show three different clusters each one containing 50 000 particles. Figure 1(a) corresponds to a simulation of a monodisperse distribution of tetra-functional monomers (1:0:0:0). This distribution reproduces the ordinary Eden model. Observe that, by sectioning the figure, we see a compact homogeneous structure (material is represented by white) with rough surface, as can be easily seen from the observation of the surface contour. The value of α obtained for this aggregate is $\alpha = 3.8 \pm 0.2$ consistent with the description of a pure Eden model. Figures 1(b) and (c) correspond to a functionality distribution of (3:3:3:1) and (0:1:1:0), respectively. Observe that holes in all length scales are present in the structure as is typical of mass fractal objects. Consistent with this description, we expect $\alpha < 3$ in both cases.

In figure 2 we have plotted in a log–log scale $S(k)$ for large k values for a few selected distributions. We include in the legend the α value computed from the best least-squares fit to the data. The complete set of data arising from our study is represented in figure 3. For the sake of clarity we have grouped the data in this figure into disjoint intervals according to the computed α value. As in experiments, we observe that the scattering behaviour is related to the water concentration. For small values of the mean functionality, $\langle n \rangle$, corresponding to low water concentration (W small), the particles are mass fractals (+ symbol in the figure). Increasing $\langle n \rangle$, the maximum value of $\sigma(n)$ is reduced. This situation corresponds to $\alpha = D_f = D_s \rightarrow d$. The cluster is not ramified enough to be considered a mass fractal but has a maximal fractal surface (∗ symbol). For bigger values of $\langle n \rangle$ the hydrolysis becomes more important and many sites are available for polymerization so that the core of the aggregates becomes homogeneous ($D_f = d$) but its variance is still large, therefore the surface remains fractal with $D_s < d$ (△ symbol). When $\langle n \rangle \rightarrow 4$, $\sigma(n) \rightarrow 0$ and $D_s \rightarrow d - 1$, as the scattering exponent $\alpha \rightarrow d + 1$ (□ symbol).

Very simple probabilistic arguments allow us to find an analytical expression relating
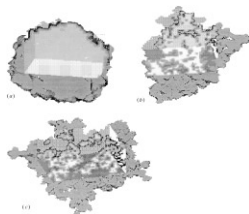

Figure 1. Silica aggregates containing 50 000 sites grown on a tetragonal lattice. (a) corresponds to a functionality distribution of (1:0:0:0); (b) to (3:3:3:1) and (c) to (0:1:1:0).

the mean functionality $\langle n \rangle$ to the W ratio. This expression allows a comparison of the simulation data with the experimental results. To do so, we shall consider P_h to be the probability that a site of the silica monomer is hydrolysed and P_u the probability that it remains poisoned when forming part of the aggregate. This differentiation is important since all monomers when forming part of the aggregate are not going to be hydrolysed anymore. Therefore, the probability of having n hydrolysed sites on a monomer belonging to the aggregate is

$$P_n = \frac{\binom{4}{n} P_h^n P_u^{4-n}}{\sum_{i=0}^{4} \binom{4}{i} P_h^i P_u^{4-i}} .$$

and the mean functionality, by definition, is

$$\langle n \rangle = \sum_{i=1}^{4} i P_i = \frac{4 P_h}{P_h + P_u} .$$

Let us assume that $P_u = \lambda$ (TEOS) and $P_h = \mu [H_2O]$, where the ratio $\mu/\lambda (= \varepsilon)$ is a parameter related to the hydrolysis capacity per water molecule. This parameter takes into
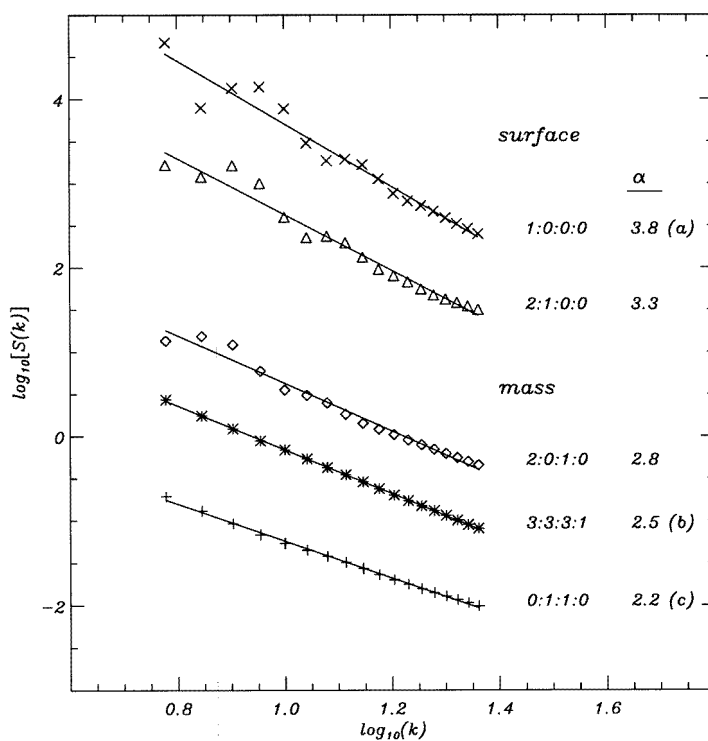

Figure 2. Log–log plot of $S(k)$ for large k values for different functionality distributions. The straight lines are the best fit to the data. The slopes of the lines yield the α value characterizing the surface fractals. (*a*)–(*c*) correspond to the pictures shown in figure 1. Each plot has been shifted by an arbitrary amount in the vertical axis for the sake of clarity.
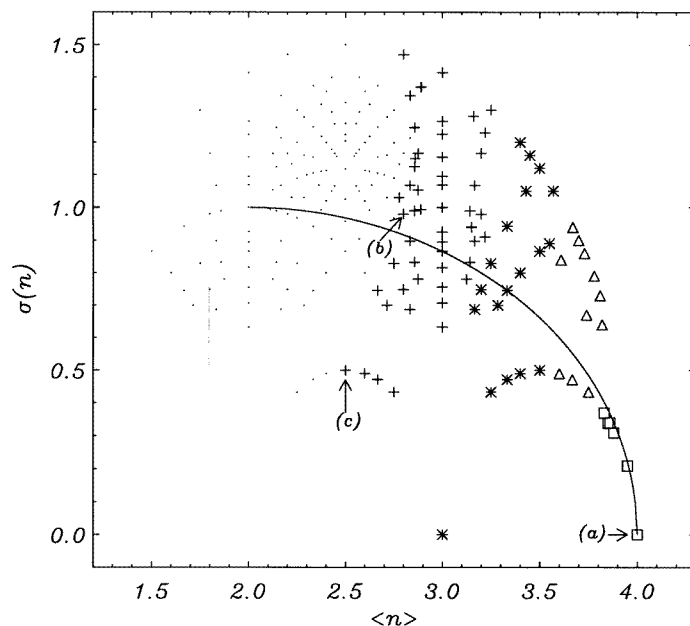
Figure 3. Representation as a function of the mean functionality $\langle n \rangle$ and its variance $\sigma(n)$ of the different α values obtained for the whole set of data gathered in disjoint intervals. The symbols refer to: 'dead' clusters ($\cdot$); mass fractals: $\alpha \leqslant 2.6$ (+), $2.6 < \alpha < 3.0$ (∗); surface fractals: $3.0 \leqslant \alpha < 3.5$ ($\triangle$), $\alpha \geqslant 3.5$ ($\square$). (*a*), (*b*) and (*c*) correspond to the pictures shown in figure 1. The full curve represents the statistically most probable experimental values of $\sigma(n)$ from (3) (see the text).

account that water molecules recovered during the polymerization process can appear several times in the hydrolysis reaction. Since $W = [H_2O]/(\text{TEOS})$ we finally get

$$\langle n \rangle = \frac{4W}{W + 1/\varepsilon} . \tag{2}$$

The asymptotic behaviour for $W \to \infty$ gives $\langle n \rangle \to 4$ as expected. To determine the unknown parameter ε we notice that for $W = 1$, the slope of the experimental curve (taken from [10]) matches, within the error bars, the numerical one corresponding to a functionality distribution of (2:0:1:0) (see figure 2), i.e. $\langle n \rangle = \frac{10}{3}$. Inserting these values in (2) we get $\varepsilon = 5$. This means that, on average, each water molecule can hydrolyse five silica monomers. In figure 4 we have represented $\langle n \rangle$ as a function of W, given by (2). We have also plotted the computed mean functionalities, whose slopes are equal to the experimental ones, corresponding to the ratios $W = 1, 2, 3, 4$. The results show good agreement between simulations and experiments.

We can also calculate the RMS of the distribution $\sigma(n)$. It is straightforward to see that

$$\sigma(n) = \sqrt{\frac{\langle n \rangle (4 - \langle n \rangle)}{4}} . \tag{3}$$

In figure 3 we have plotted $\sigma(n)$ as a function of $\langle n \rangle$ following equation (3). This curve should represent, under the probabilistic assumptions we have made, the most probable experimental values of $\sigma(n)$ for a given W.

In conclusion, we have presented in this paper extensive numerical simulations of a modified version of the Eden model. In this model, when a growth site is occupied,
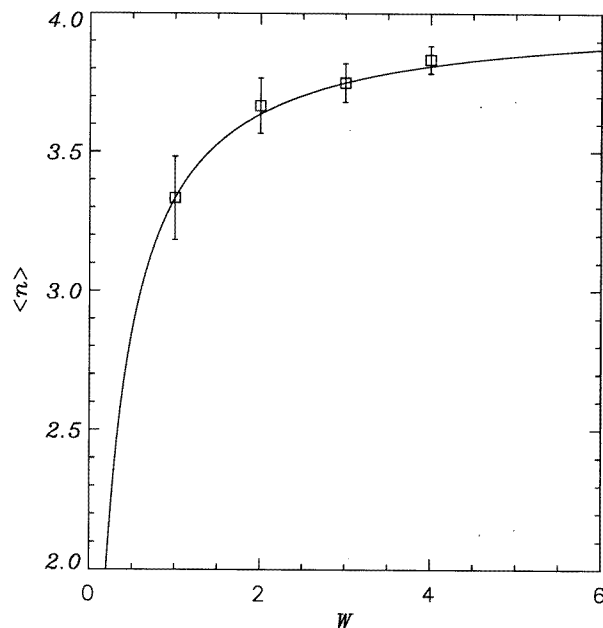
Figure 4. Plot of the mean functionality, $\langle n \rangle$, as a function of the ratio $W = [\mathrm{H_2O}]/(\mathrm{TEOS})$ given by equation (2). We also include the experimental W and computed $\langle n \rangle$ values that show the same slope, α ($\square$).

instead of designating all the adjacent vacant sites as new growth sites, some of them are poisoned and hence are prohibited from being occupied. This rule allows us to model the chemically limited nucleation and growth from incomplete hydrolysed silica monomers (TEOS). The results obtained with the proposed model are able to explain the observed correlation between the [$\mathrm{H_2O}$]:(TEOS) ratio (W) and crossover behaviour from mass fractal to surface fractal structures. We have also been able to derive an analytical expression that relates the mean functionality $\langle n \rangle$ with W. This relation, obtained using very simple probabilistic arguments, makes it possible to compare experimental and simulation data.

Acknowledgments

References

[1] Mandelbrot B B 1982 *The Fractal Geometry of Nature* (San Francisco, CA: Freeman)
[2] Avnir D (ed) 1989 *The Fractal Approach to Heterogeneous Chemistry: Surface, Colloids, Polymers* (New York: Wiley)
[3] Sinha S K 1989 *Physica* **38D** 310
[4] Guinier A and Fournet G 1955 *Small Angle Scattering of X-Rays* (New York: Wiley)

[5] Porod G 1983 *Small-Angle X-ray Scattering* ed O Glatter and O Kratky (London: Academic)

[6] Bale H D and Schmidt P W 1984 *Phys. Rev. Lett.* **53** 596

[7] Brinker C J and Scherer G W 1990 *Sol–Gel Science: The Physics and Chemistry of Sol–Gel Processing* (San Diego, CA: Academic)

[8] Hench L L and West J K 1990 *Chem. Rev.* **90** 33

[9] See, for example, Keefer K D 1984 *Mat. Res. Soc. Symp. Proc.* **32** 15

[10] Keefer K D and Schaefer D W 1986 *Phys. Rev. Lett.* **56** 2376

[11] Keefer K D 1986 *Mat. Res. Soc. Symp. Proc.* **73** 295

[12] Iler R K 1979 *The Chemistry of Silica* (New York: Wiley)

[13] Eden M 1961 *Proc. 4 Berkeley Symp. on Mathematics, Statistics, and Probability* vol 4 ed F Neyman (Berkeley, CA: University of California Press) pp 223–39

[14] Desai R C, Benard P and Corsten M 1989 *J. Phys. Chem.* **93** 6944

[15] Cao Q Z and Wong P Z 1991 *Phys. Rev. Lett.* **67** 77

[16] Keefer K D Private communication